

# $\tilde{J}$ -pseudospin states and the crystal field of cubic systems

Naoya Iwahara,<sup>1,\*</sup> Liviu Ungur,<sup>1,2</sup> and Liviu F. Chibotaru<sup>1,†</sup>

<sup>1</sup>*Theory of Nanomaterials Group, University of Leuven, Celestijnenlaan 200F, B-3001 Leuven, Belgium*

<sup>2</sup>*Department of Chemistry, National University of Singapore,  
Block S8 Level 3, 3 Science Drive 3, Singapore 117543*

(Dated: August 17, 2018)

Theory of  $\tilde{J}$ -pseudospin for  $f$  element in cubic environment is developed. By fulfilling the symmetry requirements and the adiabatic connection to atomic limit, the crystal-field states are uniquely transformed into  $\tilde{J}$ -pseudospin states. In terms of the pseudospin operators, both the total angular momentum and the crystal-field Hamiltonian contain higher-rank tensor terms than the traditional ones do, which means the present framework naturally include the effects such as the covalency and  $J$ -mixing beyond the  $f$ -shell model. Combining the developed theory with *ab initio* calculations, the  $\tilde{J}$ -pseudospin states for  $\text{Nd}^{3+}$  and  $\text{Np}^{4+}$  ions in octahedral sites of insulators are derived.

## I. INTRODUCTION

Crystal-field theory [1] has been widely used for the investigation of the electronic, magnetic, and optical properties of metal ions in complexes and solids [2, 3], and it is still intensively used [4–7]. Although the traditional electrostatic approach seems to provide basic character of the electronic structures, as is well known, it does not take account of various effects such as covalency [8, 9],  $J$ -mixing [3], and shielding [10]. To address accurately the properties of electronic states in metal ions, state-of-the-art *ab initio* quantum chemistry methodology including covalency, electron correlation, spin-orbit coupling and other relativistic effects is nowadays an alternative popular approach. Indeed, recently post Hartree-Fock methods are starting to be applied to the study of strongly correlated materials containing heavy  $d$  elements [11, 12]. A common problem of *ab initio* approaches is that the computed electronic states do not directly provide a clear physical picture. For example, in the case of magnetic systems, they are characterized in terms of pseudospin Hamiltonian [2]. While the *ab initio* states must contain all necessary information, it is not *a priori* clear how to extract the pseudospin Hamiltonian on their basis.

This issue has been recently addressed, and general principles for the derivation of the uniquely defined pseudospin Hamiltonian from *ab initio* calculated electronic states was proposed [13–15]: the principles consist of (1) symmetry requirements and (2) adiabatic connection to the well-defined limiting cases.  $N$  low-energy electronic states is selected for the description of low-energy phenomena, the  $\tilde{S}$ -pseudospin states ( $N = 2\tilde{S} + 1$ ) are derived by an unitary transformation of these electronic states and then, the pseudospin Hamiltonian is derived using the obtained pseudospin states. The unitary matrix should be uniquely determined based on these principles. There is no difficulty for the unique definition of small pseudospins ( $\tilde{S} = 1/2$  and 1): Indeed, when

only the small pseudospins are relevant, combining the theoretical framework with *ab initio* calculations, various magnetic properties of metal complexes have been explained [16, 17] and predicted [18, 19]. On the other hand, the derivation of large pseudospin  $\tilde{S} \geq 3/2$ , which is relevant to e.g.  $\tilde{J}$ -pseudospin for the crystal-field states of  $f$ -elements, remains under development [20, 21] because a practical algorithm to determine a large number of the unitary matrix elements ( $\approx N^2/2$ ) fulfilling both requirements is not obvious.

In this work, we develop the methodology to uniquely transform the crystal-field states of  $f$  elements in cubic environment into the  $\tilde{J}$ -pseudospin states satisfying the symmetry requirements and the adiabatic connection between the  $\tilde{J}$ -pseudospin states and the corresponding atomic  $J$ -multiplet. The present  $\tilde{J}$ -pseudospin states naturally include the effects beyond the traditional crystal-field model based on isolated  $f$  orbitals, resulting in the presence of the higher rank tensor terms in total angular momentum and crystal-field Hamiltonian than in conventional approaches based on atomic  $J$ -multiplet. The developed theory is applied to  $\text{Nd}^{3+}$  and  $\text{Np}^{4+}$  ions in cubic environment.

## II. UNIQUE DEFINITION OF PSEUDOSPIN

For the description of the local electronic structure and properties of magnetic ions, phenomenological pseudospin Hamiltonians are often employed [2] [22]. The pseudospin Hamiltonian acts on the abstract pseudospin states  $|\tilde{S}M\rangle$  ( $M = -\tilde{S}, -\tilde{S} + 1, \dots, \tilde{S}$ ), and its eigenstates describe the low-energy states. On the other hand, if the exact electronic states responsible for the low-energy phenomena of interest are given,

$$\mathcal{H} = \{|\Psi_i\rangle | i = 1, 2, \dots, N\}, \quad (1)$$

the pseudospin states  $|\tilde{S}M\rangle$  should be obtainable directly from this set of states. However, the relation between them is not *a priori* evident. This problem has been recently addressed by some of us and the methodology

\* naoya.iwahara@gmail.com

† liviu.chibotaru@gmail.com

to uniquely define the pseudospin states was proposed [13–15].

The pseudospin states may be obtained by unitary transformation of the electronic states  $|\Psi_i\rangle$ :

$$|\tilde{S}M\rangle = \sum_{i=1}^N U_{iM} |\Psi_i\rangle, \quad (2)$$

where,  $U_{iM}$  are elements of a unitary matrix  $U$  and  $N = 2\tilde{S} + 1$ . Once pseudospin states are established, the pseudospin operators such as

$$\tilde{S}_z = \sum_{M=-\tilde{S}}^{\tilde{S}} M |\tilde{S}M\rangle \langle \tilde{S}M|,$$

and irreducible tensor operators  $Y_{kq}(\tilde{S})$  can be assigned in their basis, where,  $k$  and  $q$  indicate the rank and the component of the tensor, respectively. Nevertheless, for an arbitrary choice of  $U$ , the obtained operators  $\tilde{S}$  would not behave as expected for the phenomenological effective spin under symmetry operations, and the obtained pseudospin Hamiltonian will also differ from the phenomenological one. In order to choose adequate unitary transformation  $U$  in Eq. (2), two requirements (principles) are employed [13–15]:

1. The pseudospin states  $|\tilde{S}M\rangle$  transform as the true spin states  $|SM\rangle$  ( $S = \tilde{S}$ ) under the time-reversal and spatial symmetry operations.
2. The pseudospin states are adiabatically connected to the well-defined pure spin/orbital/total angular momentum states.

The first principle simply requires the pseudospin states to be consistent with the symmetries of the system [2] [23]. The second principle requires the existence of the one-to-one correspondence between the pseudospin and a well-defined pure spin. This correspondence is established by adiabatically turning on the interaction which only exists in the materials [13, 15]. The latter may include covalency, spin-orbit coupling and deformation of the environment, depending on the choice of the reference situation. Such an adiabatic connection is used in various fields of condensed matter physics to characterize the systems [24, 25].

The proposed principles state the requirements for the unique definition of pseudospins, while they do not provide the practical way to achieve it. In practice, low-dimensional pseudospins ( $\tilde{S} = 1/2, 1$ ) can be uniquely defined by identifying their states with the Zeeman states along one of the principal magnetic axes of the system [14, 15]. These pseudospin states obey automatically the symmetry requirements of principle 1. On the other hand, the unique definition of larger pseudospin  $\tilde{S} \geq 3/2$  is technically more difficult than that of small pseudospins due to the quadratically increasing number of free parameters ( $\propto N^2$ ) defining the unitary transformation  $U$  in Eq. (2) [15]. If as in the small pseudospins,

the eigenstates of the magnetic moment  $\hat{\mu}_Z$  along principal magnetic axis  $Z$  are taken as pseudospin states [20], the spatial symmetry requirement may not be completely fulfilled. For example, the crystal field states of a Kramers ion in cubic environment may contain four-fold degenerate  $\Gamma_8$  states (Table I), whereas the eigenstates of  $\hat{\mu}_Z$  never do so because they satisfy at most a tetragonal symmetry under Zeeman splitting. Although the definition of the pseudospins via eigenstates of  $\hat{\mu}_Z$  is one of the possible choices, the obtained Hamiltonian will not have *a priori* the expected form for cubic system. Another issue is the requirement of the adiabatic connection: this can be in principle satisfied by defining the pseudospin by several consecutive *ab initio* calculations in which some controlling parameters are varied (see Ref. [13] and Sec. VI in Ref. [15]). It is evident that such brute force approach is far from practical for most of systems of interest. Towards the establishment of the practical scheme to determine large pseudospins, the theory of the  $\tilde{J}$ -pseudospin in cubic environment is developed below.

### III. PSEUDOSPIN IN CUBIC ENVIRONMENT

The low-energy crystal-field states of  $f$  elements mainly originate from the ground atomic  $J$ -multiplet [2]. Thus, the crystal-field Hamiltonian is described in terms of  $\tilde{J}$ -pseudospin operators. Here, the algorithm to derive the  $J$ -pseudospin crystal-field Hamiltonian in octahedral environment from the crystal-field states is shown taking  $\tilde{J} = 9/2$  pseudospin as an example because the latter is the simplest non-trivial case where both requirements in Sec. II have to be fully taken into account. Other cases can be done using the formulae in Appendix A. The developed method is applied to derive the crystal-field Hamiltonian of  $\text{Nd}^{3+}$  ( $4f^3$ ) and  $\text{Np}^{4+}$  ( $5f^3$ ) ions in octahedral environment.

#### A. $\Gamma$ -pseudospin

In an octahedral ( $O$  or  $O_h$ ) environment, the ground atomic  $J = 9/2$  multiplets split into two sets of four-fold degenerate  $\Gamma_8$  multiplets and one  $\Gamma_6$  Kramers doublet (Table I). Since the  $\Gamma_8$  and  $\Gamma_6$  states, respectively, transform as  $S = 3/2$  and  $S = 1/2$  spin states under the symmetry operations of the  $O_h$  group [27], each of the multiplets can be unambiguously transformed into  $\Gamma$ -pseudospin state by requirement 1 [ $\mathcal{H}$  corresponds to a set of degenerate  $\Gamma$  states] [15, 21]. Hereafter, the three  $C_4$  axes of the cubic environment correspond to the  $x, y, z$  axes (right-handed coordinate system), the  $z$  axis is taken as the quantization axis of the angular momentum, and the basis of the irreducible representations given in Ref. [27] is used. Using the generators of the rotational symmetry operations of the  $O_h$  group, for example,  $\pi/2$  rotations around the  $y$  and  $z$  axes ( $\hat{C}_4^y$  and  $\hat{C}_4^z$ ), the  $\Gamma$

TABLE I. The relation between  $J$ , its decomposition into  $\Gamma$  irreducible representations of cubic group  $\mathcal{G}$  ( $= O, O_h, T_d$ ), and crystal-field parameters  $B_k$  in cubic environment.  $f$ -ions (Ln: lanthanide, Ac: actinide [26]) whose ground atomic multiplets are characterized by  $J$  are also shown. Parity ( $g$  or  $u$ ) is not shown.

$J$	$f^n$	Ln	Ac	$J \downarrow \mathcal{G}$	$B_k$
0				$\Gamma_1$	-
1				$\Gamma_4$	-
2				$\Gamma_3 \oplus \Gamma_5$	$B_4$
3				$\Gamma_2 \oplus \Gamma_4 \oplus \Gamma_5$	$B_4, B_6$
4	$f^2, f^4$	$\text{Pr}^{3+}, \text{Pm}^{3+}$	$\text{U}^{4+}, \text{Np}^{3/5+}, \text{Pu}^{4/6+}$	$\Gamma_1 \oplus \Gamma_3 \oplus \Gamma_4 \oplus \Gamma_5$	$B_4, B_6, B_8$
5				$\Gamma_3 \oplus 2\Gamma_4 \oplus \Gamma_5$	$B_4, B_6, B_8, B_{10}$
6	$f^8, f^{12}$	$\text{Tb}^{3+}, \text{Tm}^{3+}$	$\text{Bk}^{3+}, \text{Cf}^{4+}$	$\Gamma_1 \oplus \Gamma_2 \oplus \Gamma_3 \oplus \Gamma_4 \oplus 2\Gamma_5$	$B_4, B_6, B_8, B_{10}, B_{12}$
7				$\Gamma_2 \oplus \Gamma_3 \oplus 2\Gamma_4 \oplus 2\Gamma_5$	$B_4, B_6, B_8, B_{10}, B_{12}, B_{14}$
8	$f^{10}$	$\text{Ho}^{3+}$	$\text{Es}^{3+}$	$\Gamma_1 \oplus 2\Gamma_3 \oplus 2\Gamma_4 \oplus 2\Gamma_5$	$B_4, B_6, B_8, B_{10}, B_{12}, B_{14}, B_{16}$
1/2				$\Gamma_6$	-
3/2				$\Gamma_8$	-
5/2	$f^1, f^5$	$\text{Ce}^{3+}, \text{Sm}^{3+}, \text{Pr}^{4+}$	$\text{Pa}^{4+}, \text{U}^{5+}, \text{Pu}^{3+}, \text{Am}^{4+}$	$\Gamma_7 \oplus \Gamma_8$	$B_4$
7/2	$f^{13}$	$\text{Yb}^{3+}$		$\Gamma_6 \oplus \Gamma_7 \oplus \Gamma_8$	$B_4, B_6$
9/2	$f^3$	$\text{Nd}^{3+}$	$\text{U}^{3+}, \text{Np}^{4+}, \text{Pu}^{5+}$	$\Gamma_6 \oplus 2\Gamma_8$	$B_4, B_6, B_8$
11/2				$\Gamma_6 \oplus \Gamma_7 \oplus 2\Gamma_8$	$B_4, B_6, B_8, B_{10}$
13/2				$\Gamma_6 \oplus 2\Gamma_7 \oplus 2\Gamma_8$	$B_4, B_6, B_8, B_{10}, B_{12}$
15/2	$f^9, f^{11}$	$\text{Dy}^{3+}, \text{Er}^{3+}$	$\text{Cf}^{3+}, \text{Es}^{2+}$	$\Gamma_6 \oplus \Gamma_7 \oplus 3\Gamma_8$	$B_4, B_6, B_8, B_{10}, B_{12}, B_{14}$

multiplets are transformed as, respectively,

$$\hat{C}_4^y |\Gamma M\rangle = \sum_{M'} d_{M'M}^{\tilde{S}} \left( \frac{\pi}{2} \right) |\Gamma M'\rangle, \quad (3)$$

and

$$\hat{C}_4^z |\Gamma M\rangle = e^{-i\frac{\pi}{2}M} |\Gamma M\rangle. \quad (4)$$

Here,  $\tilde{S} = 1/2$  for  $\Gamma = \Gamma_6$ ,  $\tilde{S} = 3/2$  for  $\Gamma = \Gamma_8$ ,  $M, M' = -\tilde{S}, -\tilde{S}+1, \dots, \tilde{S}$ , and  $d_{M'M}^{\tilde{S}}$  is the rotation matrix around the  $y$  axis (Wigner  $D$ -function) [28]. The relative phase factors between  $|\Gamma M\rangle$ 's are fixed by using time-reversal symmetry [2, 27, 29]:

$$\hat{\theta} |\Gamma M\rangle = (-1)^{\tilde{S}-M} |\Gamma, -M\rangle, \quad (5)$$

where  $\hat{\theta}$  is the time-reversal operator. Similar consideration holds for a  $T_d$  system by replacing  $C_4$  with  $S_4$ .

## B. $\tilde{J}$ -pseudospin

The  $\tilde{J}$ -pseudospin states are described by linear combinations of the  $\Gamma$ -pseudospin states [ $\mathcal{H} = \{|\Gamma M\rangle | \Gamma = \Gamma_6, \Gamma_8^{(1)}, \Gamma_8^{(2)}\}$ ]:

$$|\tilde{J}M\rangle = \sum_{\mu\Gamma M'} U_{\Gamma^{(\mu)}M', \tilde{J}M} |\Gamma^{(\mu)}M'\rangle, \quad (6)$$

where, the index  $\mu$  distinguishes the repeated  $\Gamma$  multiplets (two  $\Gamma_8$  states in the present case), and  $U_{\Gamma^{(\mu)}M', \tilde{J}M}$  are coefficients. The latter are restricted by the first requirement.  $|\tilde{J}M\rangle$  with  $M = \mp 7/2, \pm 1/2, \pm 9/2$  transform as  $|\Gamma, \pm 1/2\rangle$  under the  $C_4^z$  rotation. The relation between the  $|\tilde{J}, M\rangle$  states and  $|\Gamma_6, \pm 1/2\rangle$  states is unambiguously given by taking account of the transformations under  $C_4^y$  rotation. On the other hand, the relation between the  $|\tilde{J}M\rangle$  and two  $|\Gamma_8 \pm 1/2\rangle$  states is given up to the arbitrary mixing (rotation) of the two  $\Gamma_8$  states described by one angle  $\alpha$ . Finally, making use of the components of  $|\Gamma_8, \pm 3/2\rangle$  appearing in  $\hat{C}_4^y |\Gamma_8, \pm 1/2\rangle$ , the unitary matrix  $U$  in Eq. (6) is determined up to angle  $\alpha$ . The obtained  $\tilde{J} = 9/2$  pseudospin states are

$$\begin{aligned} \left| \tilde{J}, \mp \frac{9}{2}(\alpha) \right\rangle &= \frac{1}{2} \sqrt{\frac{3}{2}} \left| \Gamma_6, \mp \frac{1}{2} \right\rangle \mp \frac{1}{2} \sqrt{\frac{5}{2}} \left[ \cos \alpha \left| \Gamma_8^{(1)}, \mp \frac{1}{2} \right\rangle - \sin \alpha \left| \Gamma_8^{(2)}, \mp \frac{1}{2} \right\rangle \right], \\ \left| \tilde{J}, \mp \frac{7}{2}(\alpha) \right\rangle &= \frac{1}{2\sqrt{6}} \left| \Gamma_6, \pm \frac{1}{2} \right\rangle \pm \frac{1}{2} \sqrt{\frac{23}{6}} \left[ \sin(\alpha + \phi_1) \left| \Gamma_8^{(1)}, \pm \frac{1}{2} \right\rangle - \cos(\alpha + \phi_1) \left| \Gamma_8^{(2)}, \pm \frac{1}{2} \right\rangle \right], \end{aligned}$$

$$\begin{aligned}
\left| \tilde{J}, \mp \frac{5}{2}(\alpha) \right\rangle &= \pm \left[ \sin(\alpha + \phi_2) \left| \Gamma_8^{(1)}, \pm \frac{3}{2} \right\rangle + \cos(\alpha + \phi_2) \left| \Gamma_8^{(2)}, \pm \frac{3}{2} \right\rangle \right], \\
\left| \tilde{J}, \mp \frac{3}{2}(\alpha) \right\rangle &= \pm \left[ -\cos(\alpha + \phi_2) \left| \Gamma_8^{(1)}, \mp \frac{3}{2} \right\rangle + \sin(\alpha + \phi_2) \left| \Gamma_8^{(2)}, \mp \frac{3}{2} \right\rangle \right], \\
\left| \tilde{J}, \mp \frac{1}{2}(\alpha) \right\rangle &= \frac{1}{2} \sqrt{\frac{7}{3}} \left| \Gamma_6, \mp \frac{1}{2} \right\rangle \pm \frac{1}{2} \sqrt{\frac{5}{3}} \left[ \sin(\alpha + \phi_3) \left| \Gamma_8^{(1)}, \mp \frac{1}{2} \right\rangle + \cos(\alpha + \phi_3) \left| \Gamma_8^{(2)}, \mp \frac{1}{2} \right\rangle \right],
\end{aligned} \tag{7}$$

where,  $\phi_1 = \arccos \sqrt{3/115}$ ,  $\phi_2 = \arccos \sqrt{7/10}$ , and  $\phi_3 = \arccos(2/5)$ . The phase factors of  $\tilde{J}$ -pseudospin states are determined to satisfy  $\hat{\theta}|\tilde{J}M\rangle = (-1)^{\tilde{J}-M}|\tilde{J}, -M\rangle$  under time-inversion as in Eq. (5) for  $\Gamma$ -pseudospin states (see for the phase factors and time-reversal symmetry Ref. [29]). The angle  $\alpha$  is explicitly present in the left hand sides of Eq. (7) because it is not fixed yet. In addition to  $\alpha$ , there are two possibilities for the assignment of two  $\Gamma_8$  states in  $\mathcal{H}$ . By the similar procedures, all the important cases for  $f$  elements can be derived (see Appendix A).

Using the pseudospin states (7), we can define the irreducible tensor operators (Appendix B)

$$\begin{aligned}
\mathcal{Y}_{kq}(\tilde{\mathbf{J}}(\alpha)) &= \frac{Y_{kq}(\tilde{\mathbf{J}}(\alpha))}{Y_{k0}(\tilde{\mathbf{J}})} \\
&= \sum_{M, M'} \frac{\langle (\tilde{J}k)\tilde{J}M' | \tilde{J}Mkq \rangle}{\langle (\tilde{J}k)\tilde{J}\tilde{J} | \tilde{J}\tilde{J}k0 \rangle} |\tilde{J}M'(\alpha)\rangle \langle \tilde{J}M(\alpha)|.
\end{aligned} \tag{8}$$

Here,  $\tilde{\mathbf{J}}$  is the  $\tilde{J}$ -pseudospin operator,  $Y_{kq}(\tilde{\mathbf{J}})$  is the irreducible tensor operator of rank  $k$  ( $k = 0, 1, \dots, 2\tilde{J}$ ) and argument  $q$  ( $q = -k, -k + 1, \dots, k$ ),  $Y_{k0}(\tilde{\mathbf{J}}) = \langle \tilde{J}\tilde{J} | Y_{k0}(\tilde{\mathbf{J}}) | \tilde{J}\tilde{J} \rangle$ , and  $\langle (j_1 j_2) j m | j_1 m_1 j_2 m_2 \rangle$  are Clebsch-Gordan coefficients [28]. The tensor operator behaves as a pseudospin state  $|\tilde{J} = k, M = q\rangle$  under time-inversion,  $\mathcal{Y}_{kq} \rightarrow (-1)^{k-q} \mathcal{Y}_{k, -q}$ . Any electronic operators acting on the crystal-field states in  $\mathcal{H}$  can be decomposed into

$\mathcal{Y}_{kq}$ 's (see Appendix B).

For the unique definition of  $\tilde{J}$ -pseudospin, the variable  $\alpha$  in Eq. (7) has to be fixed. To this end, the second principle is used. The  $\tilde{J}$ -pseudospin states (7) and thus  $\tilde{\mathbf{J}}$  have to converge to the atomic  $J$ -multiplet and pure total angular momentum  $\hat{\mathbf{J}}$ , respectively, by adiabatically reducing the interactions with the environment. This is achieved by choosing  $\alpha$  so that the first rank parameter of  $\hat{J}_z$ ,  $j_{10}(\alpha)$ , becomes the largest:

$$\hat{J}_z = \sum_{k=1}^{2\tilde{J}} \sum_{q=-k}^k j_{kq}(\alpha) \mathcal{Y}_{kq}(\tilde{\mathbf{J}}(\alpha)). \tag{9}$$

In general,  $j_{10} < \tilde{J}$  because the degree of the mixing of the atomic  $J$ -multiplets  $|JM\rangle$  to the crystal-field states  $|\Psi_i\rangle$  depends on  $M$  owing to e.g., the covalency and  $J$ -mixing. Substituting  $\alpha_0$  maximizing  $j_{10}(\alpha)$  into Eq. (7), the  $\tilde{J}$ -pseudospin states are uniquely defined. In this procedure, all possible assignments of  $\Gamma_8$  crystal-field levels to  $\Gamma_8^{(1)}$  and  $\Gamma_8^{(2)}$  in Eq. (6) also have to be examined. If other angle  $\alpha$  such as the one at the other extremum is chosen,  $\tilde{\mathbf{J}}$  does not converge to  $\hat{\mathbf{J}}$  in the atomic limit (see Sec. III C 2) because such choice makes  $|\tilde{J}M(\alpha)\rangle$  dissimilar from  $|JM\rangle$ . The same procedure uniquely defines  $\tilde{J} \geq 9/2$ , whereas the  $\tilde{J} < 9/2$  pseudospin states are uniquely defined by symmetry.

With the use of the  $\mathcal{Y}_{kq}(\tilde{\mathbf{J}}(\alpha_0))$ , the crystal-field Hamiltonian  $\hat{H}_{cf} = \sum_{\mu \Gamma M} E_{\Gamma}^{(\mu)} |\Gamma^{(\mu)} M\rangle \langle \Gamma^{(\mu)} M|$  is expressed as (see Appendix C):

$$\hat{H}_{cf} = B_0 + B_4 \left( \mathcal{Y}_{40} + \sum_{q=\pm 4} \sqrt{\frac{5}{14}} \mathcal{Y}_{4q} \right) + B_6 \left( \mathcal{Y}_{60} - \sum_{q=\pm 4} \sqrt{\frac{7}{2}} \mathcal{Y}_{6q} \right) + B_8 \left( \mathcal{Y}_{80} + \sum_{q=\pm 4} \frac{1}{3} \sqrt{\frac{14}{11}} \mathcal{Y}_{8q} + \sum_{q=\pm 8} \frac{1}{3} \sqrt{\frac{65}{22}} \mathcal{Y}_{8q} \right), \tag{10}$$

where,  $\mathcal{Y}_{kq}(\tilde{\mathbf{J}}(\alpha_0))$  is replaced by  $\mathcal{Y}_{kq}$  for simplicity, and  $B_k$  are calculated as

$$\begin{aligned}
B_0 &= \frac{1}{10} \left[ 2E_{\Gamma_6} + 4(E_{\Gamma_8^{(1)}} + E_{\Gamma_8^{(2)}}) \right], \\
B_4 &= \frac{3}{1430} \left[ 49(2E_{\Gamma_6} - E_{\Gamma_8^{(1)}} - E_{\Gamma_8^{(2)}}) + (133 \cos 2\alpha_0 - 4\sqrt{21} \sin 2\alpha_0)(E_{\Gamma_8^{(1)}} - E_{\Gamma_8^{(2)}}) \right], \\
B_6 &= \frac{1}{220} \left[ -4(2E_{\Gamma_6} - E_{\Gamma_8^{(1)}} - E_{\Gamma_8^{(2)}}) + (8 \cos 2\alpha_0 + \sqrt{21} \sin 2\alpha_0)(E_{\Gamma_8^{(1)}} - E_{\Gamma_8^{(2)}}) \right], \\
B_8 &= \frac{1}{1040} \left[ 3(2E_{\Gamma_6} - E_{\Gamma_8^{(1)}} - E_{\Gamma_8^{(2)}}) + (-3 \cos 2\alpha_0 + 4\sqrt{21} \sin 2\alpha_0)(E_{\Gamma_8^{(1)}} - E_{\Gamma_8^{(2)}}) \right].
\end{aligned} \tag{11}$$

TABLE II. Crystal-field levels of  $\text{Cs}_2\text{NaNdCl}_6$  and  $\text{Cs}_2\text{ZrCl}_6:\text{Np}^{4+}$  ( $\text{cm}^{-1}$ )<sup>a</sup>. (a) and (b) indicate the *ab initio* methodology (Sec. III C 1) and “Exp.” the experimental data [31]. The ground  $\Gamma_8$  energy is set to zero.

$\Gamma$	Energy			
	$\text{Cs}_2\text{NaNdCl}_6$		$\text{Cs}_2\text{ZrCl}_6:\text{Np}^{4+}$	
	(a)	(b)	Exp. [31]	(a)
$\Gamma_6$	90.225	95.318	97	506.834
$\Gamma_8$	267.562	315.578	335	1352.775

<sup>a</sup>  $\Gamma_8$  levels within the method (b) are slightly split:  $0.2 \text{ cm}^{-1}$  and  $0.4 \text{ cm}^{-1}$  for the ground and excited  $\Gamma_8$  levels, respectively. In this work, the averaged values of the slightly split  $\Gamma_8$  levels were used.

Contrary to the conventional crystal-field Hamiltonian containing only fourth and sixth rank terms [30], the present one contains up to eighth rank terms (in general up to rank  $k \leq 2\tilde{J}$ ). The conventional form is recovered by imposing the constraint that all local crystal-field levels arise from the atomic  $f$  shell.

The proposed algorithm for the unique definition of  $\tilde{J}$ -pseudospin states in cubic environment is summarized as follows:

1. Express  $\tilde{J}$ -pseudospin states  $|\tilde{J}M\rangle$  using Eq. (7) or the corresponding formulae in Appendix A.
2. Maximize the first rank parameter  $j_{10}$  of  $\hat{J}_z$  (9) with respect to the free parameters.

These two procedures satisfy the principles 1 and 2 (Sec. II), respectively. With the obtained  $\tilde{J}$ -pseudospin states with the fixed angles, any operators acting on the same Hilbert space  $\mathcal{H}$  can be decomposed into the irreducible tensor operators  $\mathcal{Y}_{kq}$ 's (see Appendix B). In the next section, this algorithm is applied to two systems.

### C. *Ab initio* derivation of $\tilde{J} = 9/2$ pseudospin states

Combining the developed theory and *ab initio* calculations, the  $\tilde{J} = 9/2$  pseudospin states of  $\text{Nd}^{3+}$  ion in octahedral site of  $\text{Cs}_2\text{NaNdCl}_6$  [31] and  $\text{Np}^{4+}$  impurity ion in octahedral Zr site of  $\text{Cs}_2\text{ZrCl}_6$  [32, 33] are derived. It is also shown that the present approach fulfills the requirement 2.

#### 1. *Ab initio* method

In order to obtain the electronic structure, embedded cluster calculations were performed with a post Hartree-Fock method. For the  $\text{Cs}_2\text{NaNdCl}_6$  cluster, one  $\text{Nd}^{3+}$  ion and the nearest eight  $\text{Cl}^-$  ions are treated *ab initio*, and the distant atoms are replaced by point charges. The electronic structure was calculated using complete active

TABLE III.  $\alpha_0$  (rad), the total angular momentum  $j_{kq}$  and crystal-field parameters  $B_k$  ( $\text{cm}^{-1}$ ) of  $\text{Cs}_2\text{NaNdCl}_6$  and  $\text{Cs}_2\text{ZrCl}_6:\text{Np}^{4+}$ . (a) and (b) indicate the *ab initio* methodology (Sec. III C 1).

	$k$	$q$	$\text{Cs}_2\text{NaNdCl}_6$		$\text{Cs}_2\text{ZrCl}_6:\text{Np}^{4+}$
			(a)	(b)	(a)
$\alpha_0$			1.620	1.614	1.631
$j_{kq}$	1	0	4.455	4.452	4.242
	3	0	$6.88 \times 10^{-3}$	$9.28 \times 10^{-3}$	$2.68 \times 10^{-2}$
	5	0	$-3.15 \times 10^{-3}$	$-4.34 \times 10^{-3}$	$-1.10 \times 10^{-2}$
		$\pm 4$	$1.70 \times 10^{-4}$	$2.41 \times 10^{-3}$	$-4.54 \times 10^{-4}$
	7	0	$6.03 \times 10^{-4}$	$6.80 \times 10^{-4}$	$1.25 \times 10^{-3}$
		$\pm 4$	$-3.23 \times 10^{-4}$	$2.15 \times 10^{-4}$	$-6.15 \times 10^{-4}$
	9	0	$-3.76 \times 10^{-5}$	$-4.71 \times 10^{-5}$	$-1.12 \times 10^{-5}$
		$\pm 4$	$4.56 \times 10^{-6}$	$1.09 \times 10^{-5}$	$1.44 \times 10^{-5}$
		$\pm 8$	$3.55 \times 10^{-6}$	$8.31 \times 10^{-6}$	$1.12 \times 10^{-5}$
	$B_k$	4		-82.24	-99.53
6			-8.65	-9.74	-39.73
8			0.05	0.07	-0.22

space self-consistent field (CASSCF), extended multi-state complete active space second-order perturbation theory (XMS-CASPT2) [34, 35], and spin-orbit restricted active space state interaction (SO-RASSI) methods with atomic-natural-orbital relativistic-correlation consistent-minimal basis (ANO-RCC-MB). In the CASSCF calculations, 14 orbitals were included in the active space:  $4f$  of the  $\text{Nd}^{3+}$  ion alongside with an additional set of seven  $f$  functions (of the  $5f$  kind of the metal site). The dynamical electron correlation for these orbitals was taken into account within the XMS-CASPT2 approach. The spin-orbit coupling was taken into account with SO-RASSI method, and the scalar relativistic effects were included in the basis set. The crystal-field states of  $\text{Nd}^{3+}$  were calculated using two approaches: (a) CASSCF/SO-RASSI and (b) CASSCF/XMS-CASPT2/SO-RASSI. All calculations were performed using Molcas 8 suite of programs [36]. The crystal-field states of  $\text{Cs}_2\text{ZrCl}_6:\text{Np}^{4+}$  cluster within the same computational level were taken from the previous work [21].

#### 2. $\tilde{J}$ -pseudospins of $\text{Cs}_2\text{NaNdCl}_6$ and $\text{Cs}_2\text{ZrCl}_6:\text{Np}^{4+}$

The calculated crystal-field levels of  $\text{Cs}_2\text{NaNdCl}_6$  and  $\text{Cs}_2\text{ZrCl}_6:\text{Np}^{4+}$  clusters are given in Table II. In both cases, the irreducible representations of the crystal-field levels are  $\Gamma_8$ ,  $\Gamma_6$ ,  $\Gamma_8$  in the order of increasing energy. The obtained levels of  $\text{Cs}_2\text{NaNdCl}_6$  are in good agreement with experimental data [31], and the dynamical electron correlation makes the agreement better. The *ab initio*  $\Gamma$  multiplets were assigned by comparing the *ab initio* magnetic moment  $\hat{\mu}$  matrices and the structure of symmetry adapted model of  $\hat{\mu}$ , which also enabled us to

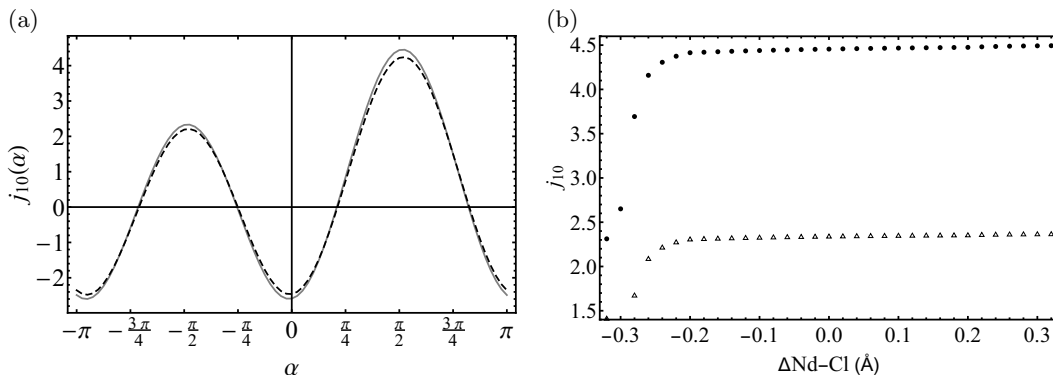


FIG. 1. (a)  $j_{10}(\alpha)$  for Nd (solid line) and Np (dashed line) clusters. (b)  $j_{10}$  of Nd cluster with respect to the totally symmetric deformation from the equilibrium Nd-Cl bond length,  $\Delta \text{Nd-Cl}$  (Å). The filled circles and open triangles indicate  $j_{10}$  with  $\alpha$  at the global maximum ( $\alpha \approx \pi/2$ ) and the local maximum ( $\alpha \approx -\pi/2$ ), respectively.

fix the relative phase factors.

Following the method in Sec. III B,  $\tilde{J} = 9/2$  pseudospin states were defined. Figure 1(a) shows the plot of  $j_{10}(\alpha)$  as a function of  $\alpha$ , and the obtained  $\alpha_0$ ,  $j_{kq}(\alpha_0)$  and  $B_k$  are listed in Table III. The  $\Gamma_8^{(1)}$  and  $\Gamma_8^{(2)}$  states in Eq. (6) correspond to the excited and the ground  $\Gamma_8$  multiplets, respectively. In order to check the principle 2,  $j_{10}$  of the Nd cluster with respect to the strength of the crystal-field which is controlled by the totally symmetric displacements of ligand atoms. Fig. 1 (b) shows  $j_{10}$  using two different  $\alpha$ : one at the maximum point ( $\alpha = \alpha_0 \approx \pi/2$ ) and the other at the second highest point ( $\alpha \approx -\pi/2$ ) in Fig. 1(a). The first one (filled circle) continues to approach the atomic limit:  $j_{10} = 4.494$  at the largest Nd-Cl. On the contrary, the second one (open triangle) remains of a much smaller value than the atomic one. This demonstrates that the pseudospin states defined by the proposed algorithm indeed fulfills the two principles outlined in Sec. II.

The coefficients  $j_{kq}$  in Table III shows that the first rank term in  $\hat{J}_z$  is dominant, whereas the higher order terms are not negligible. The discrepancy would be mainly explained by the covalency effect [20]. The effect of covalency is seen by comparing  $\text{Nd}^{3+}$  and  $\text{Np}^{4+}$  ions: due to the stronger delocalization of the  $5f$  orbital in comparison with the  $4f$  orbital, the bonding to the ligand becomes more important in the former, which results in a stronger reduction of  $j_{10}$  in  $\text{Np}^{4+}$  than in  $\text{Nd}^{3+}$ . The discrepancy between the traditional crystal-field approach [30] and the *ab initio* wave function based treatment described here also arises in the form of the crystal-field Hamiltonian, which involves as eighth-rank terms in the latter case. We stress that the  $\tilde{J}$ -pseudospin Hamiltonian is more exact because, being derived directly from the *ab initio* electronic states, it reproduces by definition not only their energies but also all their electronic properties.

#### IV. DISCUSSION

The present  $\tilde{J}$ -pseudospin states fulfill both requirements presented in Sec. II. The same methodology will apply to other cases. For  $\tilde{J} < 9/2$ , the pseudospin states are uniquely defined by using the first principle as shown in Appendix A, whereas there are a few arbitrary parameters in the case of  $\tilde{J} \geq 9/2$ . The mixing parameters have to be introduced because some  $\Gamma$  representations of the cubic group appear more than once under the descent of symmetry,  $\tilde{J} \downarrow O_h$  (see Table I and Appendix A).

One also should note that the present definition is one of the many equivalent definitions. In the case of octahedral systems, the eigenstates of  $\hat{\mu}_z$  cannot be used as the pseudospin states which satisfy the symmetry requirements. This is explained by the fact that the applied magnetic field (Zeeman interaction) lowers the symmetry to and the eigenstates fulfill at most tetragonal symmetry. Similar situation arises in all systems of cubic or icosahedral symmetry. In such cases, the idea of the approach proposed here should be applied. On the other hand, if the system has a low symmetry which in practice cannot be adiabatically changed into the cubic or higher one and the Zeeman interaction does not lower the symmetry, the conventional definition using the eigenstates of  $\hat{\mu}_z$  [20] will be reasonable.

In Sec. III C, to check the adiabatic connection between the obtained  $\tilde{J}$ -pseudospin states in cubic symmetry and atomic  $J$ -multiplets, *ab initio* calculations were performed at many cubic structures. However, this procedure could be significantly simplified by applying the indicator function approach proposed in Ref. [15]. With this method, the information of the atomic limit will be extracted from the wave function of the embedded system.

## V. CONCLUSIONS

In this work, the theory of  $\tilde{J}$ -pseudospin for cubic systems is developed. Using the symmetry, we derived the analytical expressions for all important  $\tilde{J}$ -pseudospin states. Despite the high spatial and time-reversal symmetries, the large- $\tilde{J}$  pseudospin states cannot be completely determined due to the presence of the several arbitrary parameters. These free parameters are fixed by using the requirement of adiabatic connection. In the case of  $\tilde{J}$ -pseudospin for the crystal-field model of  $f$  elements, the free parameter is determined by maximizing the first rank term of total angular momentum because this definition allows  $\tilde{J}$ -pseudospin to converge to pure total angular momentum in the atomic limit. Although the original idea to fulfill the second requirement of the adiabatic connection is by performing many consecutive *ab initio* calculations varying the strength of interaction, the present algorithm enables us to determine the  $\tilde{J}$ -pseudospin based only on one calculation. With the derived  $\tilde{J}$ -pseudospin states, the total angular momentum and the crystal-field Hamiltonian contain terms of higher rank than fourth and sixth, which do not exist in the conventional model based on  $f$ -shells. The discrepancy can arise due to the effects which are not contained within the atomic shell model. Combining the developed approach and *ab initio* calculations, the crystal-field Hamiltonian of the  $\text{Nd}^{3+}$  and  $\text{Np}^{4+}$  ions in cubic environment were successfully derived. Finally, we emphasize that the current methodology is not specific to the method for the calculations of wave functions, and is applicable to any multiplet states. Thus, with the increase of the accuracy of the *ab initio* calculations, accurate definition of

pseudospins can be achieved.

## ACKNOWLEDGMENT

N.I. was supported by Japan Society for the Promotion of Science Overseas Research Fellowship.

### Appendix A: $\tilde{J}$ pseudospin states

The relation between the  $\tilde{J}$  pseudospin states and  $\Gamma$  crystal-field states,

$$(|\Gamma\gamma\rangle, |\Gamma'\gamma'\rangle, \dots) = (|M\rangle, |M'\rangle, \dots)U, \quad (\text{A1})$$

is derived up to  $J = 8$ , where,  $(|\Gamma\gamma\rangle, \dots)$  and  $(|M\rangle, \dots)$  are indices of crystal-field states and  $\tilde{J}$ -pseudospin states, respectively,  $U$  is orthogonal matrix, and  $|M\rangle$  stands for  $|\tilde{J}M\rangle$ . The basis of the irreducible representations of cubic symmetry are taken from Ref. [27], and  $|\tilde{J}M\rangle$  transform as spherical harmonics [28]. The procedure of the derivation is similar to that of  $\tilde{J} = 9/2$  pseudospin states (Sec. III). The transformation coefficients  $U$  between the non-repeating  $\Gamma$  states (Table I) and the  $\tilde{J}$ -pseudospin states are unambiguously determined by symmetry. The other  $\Gamma$  states are determined up to their linear combinations, which are described by using the rotational matrices [28]:

$$R^{(2)}(\alpha) = \begin{pmatrix} \cos \alpha & -\sin \alpha \\ \sin \alpha & \cos \alpha \end{pmatrix}, \quad (\text{A2})$$

and

$$R^{(3)}(\Omega) = \begin{pmatrix} \cos \alpha \cos \beta \cos \gamma - \sin \alpha \sin \gamma & -\cos \alpha \cos \beta \sin \gamma - \sin \alpha \cos \gamma & \cos \alpha \sin \beta \\ \sin \alpha \cos \beta \cos \gamma + \cos \alpha \sin \gamma & -\sin \alpha \cos \beta \sin \gamma + \cos \alpha \cos \gamma & \sin \alpha \sin \beta \\ -\sin \beta \cos \gamma & \sin \beta \sin \gamma & \cos \beta \end{pmatrix}, \quad (\text{A3})$$

where,  $\alpha, \beta, \gamma$  are angles, and  $\Omega = (\alpha, \beta, \gamma)$ . For the description of the  $\tilde{J}$ -pseudospin states of non-Kramers systems, symmetric and antisymmetric states are sometimes used: for positive  $M = m$  ( $m \leq \tilde{J}$ ),

$$|m_{\pm}\rangle = \frac{1}{\sqrt{2}} (|-m\rangle \pm |+m\rangle). \quad (\text{A4})$$

### 1. Non-Kramers ion

#### a. $\tilde{J} = 2$

$$|\Gamma_3\theta\rangle = |0\rangle, \quad |\Gamma_3\epsilon\rangle = |2_+\rangle, \quad |\Gamma_5, 0\rangle = |2_-\rangle, \quad |\Gamma_5, \mp 1\rangle = |\pm|\pm 1\rangle. \quad (\text{A5})$$

The crystal-field parameter  $B_4$  is given by

$$B_4 = \frac{E_{\Gamma_3} - E_{\Gamma_5}}{10}. \quad (\text{A6})$$

b.  $\tilde{J} = 3$

$$\begin{aligned}
& (|\Gamma_2\rangle, |\Gamma_4, 0\rangle, |\Gamma_4, -1\rangle, |\Gamma_4, +1\rangle, |\Gamma_5, 0\rangle, |\Gamma_5, -1\rangle, |\Gamma_5, +1\rangle) \\
& = (|2_-\rangle, |0\rangle, |2_+\rangle, |-1\rangle, |+3\rangle, |+1\rangle, |-3\rangle) \\
& \quad \times \begin{pmatrix} 1 & 0 & 0 & 0 & 0 & 0 & 0 \\ 0 & 1 & 0 & 0 & 0 & 0 & 0 \\ 0 & 0 & 0 & 0 & 1 & 0 & 0 \\ 0 & 0 & M_1 & 0 & 0 & 0 & M_2 \\ 0 & 0 & 0 & M_1 & 0 & M_2 & 0 \end{pmatrix}, \tag{A7}
\end{aligned}$$

where,

$$M_1 = \begin{pmatrix} -\frac{1}{2}\sqrt{\frac{3}{2}} \\ -\frac{1}{2}\sqrt{\frac{5}{2}} \end{pmatrix}, \quad M_2 = \begin{pmatrix} \frac{1}{2}\sqrt{\frac{5}{2}} \\ -\frac{1}{2}\sqrt{\frac{3}{2}} \end{pmatrix}. \tag{A8}$$

The crystal-field parameters are

$$B_4 = \frac{-6E_{\Gamma_2} + 9E_{\Gamma_4} - 3E_{\Gamma_5}}{44}, \quad B_6 = \frac{-4E_{\Gamma_2} - 5E_{\Gamma_4} + 9E_{\Gamma_5}}{616}. \tag{A9}$$

c.  $\tilde{J} = 4$

$$\begin{aligned}
& (|\Gamma_1\rangle, |\Gamma_3\theta\rangle, |\Gamma_3\epsilon\rangle, |\Gamma_4, 0\rangle, |\Gamma_4, -1\rangle, |\Gamma_4, +1\rangle, |\Gamma_5, 0\rangle, |\Gamma_5, -1\rangle, |\Gamma_5, +1\rangle) \\
& = (|4_+\rangle, |0\rangle, |2_+\rangle, |4_-\rangle, |2_-\rangle, |-1\rangle, |+3\rangle, |+1\rangle, |-3\rangle) \\
& \quad \times \begin{pmatrix} \frac{1}{2}\sqrt{\frac{5}{3}} & -\frac{1}{2}\sqrt{\frac{7}{3}} & 0 & 0 & 0 & 0 & 0 & 0 & 0 \\ \frac{1}{2}\sqrt{\frac{7}{3}} & \frac{1}{2}\sqrt{\frac{5}{3}} & 0 & 0 & 0 & 0 & 0 & 0 & 0 \\ 0 & 0 & -1 & 0 & 0 & 0 & 0 & 0 & 0 \\ 0 & 0 & 0 & 1 & 0 & 0 & 0 & 0 & 0 \\ 0 & 0 & 0 & 0 & 0 & 0 & 1 & 0 & 0 \\ 0 & 0 & 0 & 0 & -M_1 & 0 & 0 & 0 & -M_2 \\ 0 & 0 & 0 & 0 & 0 & M_1 & 0 & M_2 & 0 \end{pmatrix}, \tag{A10}
\end{aligned}$$

where,

$$M_1 = \frac{1}{2\sqrt{2}} \begin{pmatrix} \sqrt{7} \\ 1 \end{pmatrix}, \quad M_2 = \frac{1}{2\sqrt{2}} \begin{pmatrix} -1 \\ \sqrt{7} \end{pmatrix}. \tag{A11}$$

The crystal-field parameters are given by

$$\begin{aligned}
B_4 & = \frac{7(14E_{\Gamma_1} + 4E_{\Gamma_3} + 21E_{\Gamma_4} - 39E_{\Gamma_5})}{858}, \quad B_6 = \frac{-20E_{\Gamma_1} + 32E_{\Gamma_3} + 3(E_{\Gamma_4} - 5E_{\Gamma_5})}{990}, \\
B_8 & = \frac{5E_{\Gamma_1} + 7E_{\Gamma_3} - 12E_{\Gamma_4}}{1560}. \tag{A12}
\end{aligned}$$

d.  $\tilde{J} = 5$

$$\begin{aligned}
& (|\Gamma_3\theta\rangle, |\Gamma_3\epsilon\rangle, |\Gamma_4^{(1)}, 0\rangle, |\Gamma_4^{(2)}, 0\rangle, |\Gamma_4^{(1)}, -1\rangle, |\Gamma_4^{(2)}, -1\rangle, |\Gamma_4^{(1)}, +1\rangle, |\Gamma_4^{(2)}, +1\rangle, |\Gamma_5, 0\rangle, |\Gamma_5, -1\rangle, |\Gamma_5, +1\rangle) \\
& = (|4_-\rangle, |2_-\rangle, |4_+\rangle, |0\rangle, |2_+\rangle, |-5\rangle, |-1\rangle, |+3\rangle, |+5\rangle, |+1\rangle, |-3\rangle) \\
& \quad \times \begin{pmatrix} 1 & 0 & 0 & 0 & 0 & 0 & 0 & 0 & 0 \\ 0 & -1 & 0 & 0 & 0 & 0 & 0 & 0 & 0 \\ 0 & 0 & R^{(2)}(\alpha) & 0 & 0 & 0 & 0 & 0 & 0 \\ 0 & 0 & 0 & 0 & 0 & 0 & 1 & 0 & 0 \\ 0 & 0 & 0 & M_1 R^{(2)}(\alpha) & 0 & 0 & 0 & 0 & M_2 \\ 0 & 0 & 0 & 0 & M_1 R^{(2)}(\alpha) & 0 & M_2 & 0 & 0 \end{pmatrix}, \tag{A13}
\end{aligned}$$



where,  $M_1$  and  $M_2$  are defined by

$$M_1 = \frac{1}{8\sqrt{2}} \begin{pmatrix} \sqrt{5} & 3\sqrt{7} \\ \sqrt{42} & \sqrt{30} \\ -9 & \sqrt{35} \end{pmatrix}, \quad M_2 = \frac{1}{4\sqrt{2}} \begin{pmatrix} \sqrt{15} \\ -\sqrt{14} \\ -\sqrt{3} \end{pmatrix}. \quad (\text{A14})$$

*e.*  $\tilde{J} = 6$

$$\begin{aligned} & \left( |\Gamma_1\rangle, |\Gamma_2\rangle, |\Gamma_3\theta\rangle, |\Gamma_3\epsilon\rangle, |\Gamma_4, 0\rangle, |\Gamma_4, -1\rangle, |\Gamma_4, +1\rangle, |\Gamma_5^{(1)}, 0\rangle, |\Gamma_5^{(2)}, 0\rangle, |\Gamma_5^{(1)}, -1\rangle, |\Gamma_5^{(2)}, -1\rangle, |\Gamma_5^{(1)}, +1\rangle, |\Gamma_5^{(2)}, +1\rangle \right) \\ & = (|4_+\rangle, |0\rangle, |6_+\rangle, |2_+\rangle, |4_-\rangle, |6_-\rangle, |2_-\rangle, |-5\rangle, |-1\rangle, |+3\rangle, |+5\rangle, |+1\rangle, |-3\rangle) \\ & \times \begin{pmatrix} \frac{1}{2}\sqrt{\frac{7}{2}} & 0 & \frac{1}{2\sqrt{2}} & 0 & 0 & 0 & 0 & 0 & 0 & 0 & 0 \\ -\frac{1}{2\sqrt{2}} & 0 & \frac{1}{2}\sqrt{\frac{7}{2}} & 0 & 0 & 0 & 0 & 0 & 0 & 0 & 0 \\ 0 & \frac{\sqrt{5}}{4} & 0 & \frac{\sqrt{11}}{4} & 0 & 0 & 0 & 0 & 0 & 0 & 0 \\ 0 & -\frac{\sqrt{11}}{4} & 0 & \frac{\sqrt{5}}{4} & 0 & 0 & 0 & 0 & 0 & 0 & 0 \\ 0 & 0 & 0 & 0 & 1 & 0 & 0 & 0 & 0 & 0 & 0 \\ 0 & 0 & 0 & 0 & 0 & 0 & 0 & R^{(2)}(\alpha) & 0 & 0 & 0 \\ 0 & 0 & 0 & 0 & 0 & M_1 & 0 & 0 & 0 & 0 & M_2 R^{(2)}(\alpha) \\ 0 & 0 & 0 & 0 & 0 & 0 & -M_1 & 0 & -M_2 R^{(2)}(\alpha) & 0 & 0 \end{pmatrix} \quad (\text{A15}) \end{aligned}$$

where,

$$M_1 = \frac{1}{4\sqrt{2}} \begin{pmatrix} -\sqrt{11} \\ \sqrt{6} \\ -\sqrt{15} \end{pmatrix}, \quad M_2 = \frac{1}{16} \begin{pmatrix} \sqrt{3} & \sqrt{165} \\ 3\sqrt{22} & \sqrt{10} \\ \sqrt{55} & -9 \end{pmatrix}. \quad (\text{A16})$$

*f.*  $\tilde{J} = 7$

$$\begin{aligned} & \left( |\Gamma_2\rangle, |\Gamma_3\theta\rangle, |\Gamma_3\epsilon\rangle, |\Gamma_4^{(1)}, 0\rangle, |\Gamma_4^{(2)}, 0\rangle, |\Gamma_4^{(1)}, -1\rangle, |\Gamma_4^{(2)}, -1\rangle, |\Gamma_4^{(1)}, +1\rangle, |\Gamma_4^{(2)}, +1\rangle, |\Gamma_5^{(1)}, 0\rangle, |\Gamma_5^{(2)}, 0\rangle, \right. \\ & \quad \left. |\Gamma_5^{(1)}, -1\rangle, |\Gamma_5^{(2)}, -1\rangle, |\Gamma_5^{(1)}, +1\rangle, |\Gamma_5^{(2)}, +1\rangle \right) \\ & = (|6_-\rangle, |2_-\rangle, |4_-\rangle, |4_+\rangle, |0\rangle, |6_+\rangle, |2_+\rangle, |-5\rangle, |-1\rangle, |+3\rangle, |+7\rangle, |+5\rangle, |+1\rangle, |-3\rangle, |-7\rangle) \\ & \times \begin{pmatrix} \frac{1}{2}\sqrt{\frac{11}{6}} & 0 & -\frac{1}{2}\sqrt{\frac{13}{6}} & 0 & 0 & 0 & 0 & 0 & 0 & 0 & 0 \\ \frac{1}{2}\sqrt{\frac{13}{6}} & 0 & \frac{1}{2}\sqrt{\frac{11}{6}} & 0 & 0 & 0 & 0 & 0 & 0 & 0 & 0 \\ 0 & 1 & 0 & 0 & 0 & 0 & 0 & 0 & 0 & 0 & 0 \\ 0 & 0 & 0 & R^{(2)}(\alpha) & 0 & 0 & 0 & 0 & 0 & 0 & 0 \\ 0 & 0 & 0 & 0 & 0 & 0 & R^{(2)}(\beta) & 0 & 0 & 0 & 0 \\ 0 & 0 & 0 & 0 & M_1 R^{(2)}(\alpha) & 0 & 0 & 0 & 0 & M_2 R^{(2)}(\beta) & 0 \\ 0 & 0 & 0 & 0 & 0 & M_1 R^{(2)}(\alpha) & 0 & M_2 R^{(2)}(\beta) & 0 & 0 & 0 \end{pmatrix}, \quad (\text{A17}) \end{aligned}$$

where,

$$M_1 = \frac{1}{32} \begin{pmatrix} 25 & -\sqrt{231} \\ -3\sqrt{33} & -5\sqrt{7} \\ \sqrt{11} & -3\sqrt{21} \\ -\sqrt{91} & -\sqrt{429} \end{pmatrix}, \quad M_2 = \frac{1}{32\sqrt{2}} \begin{pmatrix} 5\sqrt{13} & \sqrt{11} \\ \sqrt{429} & 15\sqrt{3} \\ -3\sqrt{143} & 19 \\ -\sqrt{7} & -\sqrt{1001} \end{pmatrix}. \quad (\text{A18})$$

*g.*  $\tilde{J} = 8$

$$\begin{aligned}
& \left( |\Gamma_1\rangle, |\Gamma_3^{(1)}\theta\rangle, |\Gamma_3^{(2)}\theta\rangle, |\Gamma_3^{(1)}\epsilon\rangle, |\Gamma_3^{(2)}\epsilon\rangle, |\Gamma_4^{(1)}, 0\rangle, |\Gamma_4^{(2)}, 0\rangle, |\Gamma_4^{(1)}, -1\rangle, |\Gamma_4^{(2)}, -1\rangle, |\Gamma_4^{(1)}, +1\rangle, |\Gamma_4^{(2)}, +1\rangle, |\Gamma_5^{(1)}, 0\rangle, |\Gamma_5^{(2)}, 0\rangle, \right. \\
& \qquad \qquad \qquad \left. |\Gamma_5^{(1)}, -1\rangle, |\Gamma_5^{(2)}, -1\rangle, |\Gamma_5^{(1)}, +1\rangle, |\Gamma_5^{(2)}, +1\rangle \right) \\
& = (|8_+\rangle, |4_+\rangle, |0\rangle, |6_+\rangle, |2_+\rangle, |8_-\rangle, |4_-\rangle, |6_-\rangle, |2_-\rangle, |-5\rangle, |-1\rangle, |+3\rangle, |+7\rangle, |+5\rangle, |+1\rangle, |-3\rangle, |-7\rangle) \\
& \times \begin{pmatrix} M_1 & M_2 R^{(2)}(\alpha) & 0 & 0 & 0 & 0 & 0 & 0 & 0 & 0 \\ 0 & 0 & M_3 M_2 R^{(2)}(\alpha) & 0 & 0 & 0 & 0 & 0 & 0 & 0 \\ 0 & 0 & 0 & R^{(2)}(\beta) & 0 & 0 & 0 & 0 & 0 & 0 \\ 0 & 0 & 0 & 0 & 0 & 0 & R^{(2)}(\gamma) & 0 & 0 & 0 \\ 0 & 0 & 0 & 0 & -M_4 R^{(2)}(\beta) & 0 & 0 & 0 & 0 & -M_5 R^{(2)}(\gamma) \\ 0 & 0 & 0 & 0 & 0 & M_4 R^{(2)}(\beta) & 0 & M_5 R^{(2)}(\gamma) & 0 & 0 \end{pmatrix}, \tag{A19}
\end{aligned}$$

where,

$$\begin{aligned}
M_1 &= \frac{1}{8\sqrt{3}} \begin{pmatrix} \sqrt{65} \\ 2\sqrt{7} \\ 3\sqrt{11} \end{pmatrix}, \quad M_2 = \frac{1}{8\sqrt{93}} \begin{pmatrix} \sqrt{2145} & -16\sqrt{7} \\ 2\sqrt{231} & 8\sqrt{65} \\ -31\sqrt{3} & 0 \end{pmatrix}, \quad M_3 = \frac{1}{96} \begin{pmatrix} 3\sqrt{10} & 6\sqrt{182} & -3\sqrt{286} \\ \sqrt{6006} & -2\sqrt{330} & -3\sqrt{210} \end{pmatrix}, \\
M_4 &= \frac{1}{32} \begin{pmatrix} \sqrt{35} & 3\sqrt{13} \\ \sqrt{715} & \sqrt{77} \\ \sqrt{273} & -5\sqrt{15} \\ 1 & \sqrt{455} \end{pmatrix}, \quad M_5 = \frac{1}{32\sqrt{2}} \begin{pmatrix} 7\sqrt{21} & -\sqrt{715} \\ -\sqrt{429} & -\sqrt{35} \\ \sqrt{455} & 3\sqrt{33} \\ 3\sqrt{15} & \sqrt{1001} \end{pmatrix}. \tag{A20}
\end{aligned}$$

## 2. Kramers ion

*a.*  $\tilde{J} = 5/2$

$$\begin{aligned}
& \left( \left| \Gamma_7, -\frac{1}{2} \right\rangle, \left| \Gamma_7, +\frac{1}{2} \right\rangle, \left| \Gamma_8, -\frac{3}{2} \right\rangle, \left| \Gamma_8, +\frac{3}{2} \right\rangle, \left| \Gamma_8, -\frac{1}{2} \right\rangle, \left| \Gamma_8, +\frac{1}{2} \right\rangle \right) \\
& = \left( \left| -\frac{5}{2} \right\rangle, \left| +\frac{3}{2} \right\rangle, \left| +\frac{5}{2} \right\rangle, \left| -\frac{3}{2} \right\rangle, \left| -\frac{1}{2} \right\rangle, \left| +\frac{1}{2} \right\rangle \right) \begin{pmatrix} M_1 & 0 & 0 & M_2 & 0 & 0 \\ 0 & M_1 & M_2 & 0 & 0 & 0 \\ 0 & 0 & 0 & 0 & 1 & 0 \\ 0 & 0 & 0 & 0 & 0 & 1 \end{pmatrix}, \tag{A21}
\end{aligned}$$

where,

$$M_1 = \begin{pmatrix} \frac{1}{\sqrt{6}} \\ -\sqrt{\frac{5}{6}} \end{pmatrix}, \quad M_2 = \begin{pmatrix} \sqrt{\frac{5}{6}} \\ \frac{1}{\sqrt{6}} \end{pmatrix}. \tag{A22}$$

The crystal-field parameter is given by

$$B_4 = -\frac{E_{\Gamma_7} - E_{\Gamma_8}}{6}. \tag{A23}$$

b.  $\tilde{J} = 7/2$

$$\begin{aligned}
& \left( \left| \Gamma_6, -\frac{1}{2} \right\rangle, \left| \Gamma_6, +\frac{1}{2} \right\rangle, \left| \Gamma_7, -\frac{1}{2} \right\rangle, \left| \Gamma_7, +\frac{1}{2} \right\rangle, \left| \Gamma_8, -\frac{1}{2} \right\rangle, \left| \Gamma_8, +\frac{1}{2} \right\rangle, \left| \Gamma_8, -\frac{3}{2} \right\rangle, \left| \Gamma_8, +\frac{3}{2} \right\rangle \right) \\
&= \left( \left| +\frac{7}{2} \right\rangle, \left| -\frac{1}{2} \right\rangle, \left| -\frac{7}{2} \right\rangle, \left| +\frac{1}{2} \right\rangle, \left| -\frac{5}{2} \right\rangle, \left| +\frac{3}{2} \right\rangle, \left| +\frac{5}{2} \right\rangle, \left| -\frac{3}{2} \right\rangle \right) \\
&\quad \times \begin{pmatrix} M_1 & 0 & 0 & 0 & M_3 & 0 & 0 & 0 \\ 0 & -M_1 & 0 & 0 & 0 & M_3 & 0 & 0 \\ 0 & 0 & M_2 & 0 & 0 & 0 & 0 & M_4 \\ 0 & 0 & 0 & -M_2 & 0 & 0 & M_4 & 0 \end{pmatrix}, \tag{A24}
\end{aligned}$$

where,

$$M_1 = \begin{pmatrix} \frac{1}{2}\sqrt{\frac{5}{3}} \\ \frac{1}{2}\sqrt{\frac{7}{3}} \end{pmatrix}, \quad M_2 = \begin{pmatrix} -\frac{\sqrt{3}}{2} \\ \frac{1}{2} \end{pmatrix}, \quad M_3 = \begin{pmatrix} -\frac{1}{2}\sqrt{\frac{7}{3}} \\ \frac{1}{2}\sqrt{\frac{5}{3}} \end{pmatrix}, \quad M_4 = \begin{pmatrix} -\frac{1}{2} \\ -\frac{\sqrt{3}}{2} \end{pmatrix}. \tag{A25}$$

The crystal-field parameters are calculated as

$$B_4 = \frac{49E_{\Gamma_6} - 63E_{\Gamma_7} + 14E_{\Gamma_8}}{264}, \quad B_6 = \frac{-5E_{\Gamma_6} - 3E_{\Gamma_7} + 8E_{\Gamma_8}}{264}. \tag{A26}$$

c.  $\tilde{J} = 9/2$

$$\begin{aligned}
& \left( \left| \Gamma_6, -\frac{1}{2} \right\rangle, \left| \Gamma_6, +\frac{1}{2} \right\rangle, \left| \Gamma_8^{(1)}, -\frac{1}{2} \right\rangle, \left| \Gamma_8^{(2)}, -\frac{1}{2} \right\rangle, \left| \Gamma_8^{(1)}, +\frac{1}{2} \right\rangle, \left| \Gamma_8^{(2)}, +\frac{1}{2} \right\rangle, \left| \Gamma_8^{(1)}, -\frac{3}{2} \right\rangle, \left| \Gamma_8^{(2)}, -\frac{3}{2} \right\rangle, \right. \\
&\quad \left. \left| \Gamma_8^{(1)}, +\frac{3}{2} \right\rangle, \left| \Gamma_8^{(2)}, +\frac{3}{2} \right\rangle \right) \\
&= \left( \left| +\frac{7}{2} \right\rangle, \left| -\frac{1}{2} \right\rangle, \left| -\frac{9}{2} \right\rangle, \left| -\frac{7}{2} \right\rangle, \left| +\frac{1}{2} \right\rangle, \left| +\frac{9}{2} \right\rangle, \left| -\frac{5}{2} \right\rangle, \left| +\frac{3}{2} \right\rangle, \left| +\frac{5}{2} \right\rangle, \left| -\frac{3}{2} \right\rangle \right) \\
&\quad \times \begin{pmatrix} M_1 & 0 & M_2 R^{(2)}(\alpha) & 0 & 0 & 0 \\ 0 & M_1 & 0 & -M_2 R^{(2)}(\alpha) & 0 & 0 \\ 0 & 0 & 0 & 0 & 0 & M_3 M_2 R^{(2)}(\alpha) \\ 0 & 0 & 0 & 0 & -M_3 M_2 R^{(2)}(\alpha) & 0 \end{pmatrix}, \tag{A27}
\end{aligned}$$

where,

$$M_1 = \frac{1}{2\sqrt{6}} \begin{pmatrix} 1 \\ \sqrt{14} \\ 3 \end{pmatrix}, \quad M_2 = \frac{1}{2\sqrt{30}} \begin{pmatrix} \sqrt{3} & -4\sqrt{7} \\ \sqrt{42} & 2\sqrt{2} \\ -5\sqrt{3} & 0 \end{pmatrix}, \quad M_3 = \frac{1}{4\sqrt{6}} \begin{pmatrix} -5\sqrt{2} & 2\sqrt{7} & -3\sqrt{2} \\ \sqrt{42} & 2\sqrt{3} & -\sqrt{42} \end{pmatrix}. \tag{A28}$$

d.  $\tilde{J} = 11/2$

$$\begin{aligned}
& \left( \left| \Gamma_6, -\frac{1}{2} \right\rangle, \left| \Gamma_6, +\frac{1}{2} \right\rangle, \left| \Gamma_7, -\frac{1}{2} \right\rangle, \left| \Gamma_7, +\frac{1}{2} \right\rangle, \left| \Gamma_8^{(1)}, -\frac{1}{2} \right\rangle, \left| \Gamma_8^{(2)}, -\frac{1}{2} \right\rangle, \left| \Gamma_8^{(1)}, +\frac{1}{2} \right\rangle, \left| \Gamma_8^{(2)}, +\frac{1}{2} \right\rangle, \right. \\
&\quad \left. \left| \Gamma_8^{(1)}, -\frac{3}{2} \right\rangle, \left| \Gamma_8^{(2)}, -\frac{3}{2} \right\rangle, \left| \Gamma_8^{(1)}, +\frac{3}{2} \right\rangle, \left| \Gamma_8^{(2)}, +\frac{3}{2} \right\rangle \right) \\
&= \left( \left| +\frac{7}{2} \right\rangle, \left| -\frac{1}{2} \right\rangle, \left| -\frac{9}{2} \right\rangle, \left| -\frac{7}{2} \right\rangle, \left| +\frac{1}{2} \right\rangle, \left| +\frac{9}{2} \right\rangle, \left| -\frac{5}{2} \right\rangle, \left| +\frac{3}{2} \right\rangle, \left| +\frac{11}{2} \right\rangle, \left| +\frac{5}{2} \right\rangle, \left| -\frac{3}{2} \right\rangle, \left| -\frac{11}{2} \right\rangle \right) \\
&\quad \times \begin{pmatrix} M_1 & 0 & 0 & 0 & M_3 R^{(2)}(\beta) & 0 & 0 & 0 \\ 0 & -M_1 & 0 & 0 & 0 & M_3 R^{(2)}(\beta) & 0 & 0 \\ 0 & 0 & M_2 & 0 & 0 & 0 & 0 & M_4 M_3 R^{(2)}(\beta) \\ 0 & 0 & 0 & -M_2 & 0 & 0 & M_4 M_3 R^{(2)}(\beta) & 0 \end{pmatrix}, \tag{A29}
\end{aligned}$$

where,

$$M_1 = \frac{1}{4\sqrt{3}} \begin{pmatrix} \sqrt{35} \\ -\sqrt{6} \\ \sqrt{7} \end{pmatrix}, \quad M_2 = \frac{1}{4\sqrt{3}} \begin{pmatrix} \sqrt{11} \\ \sqrt{22} \\ -\sqrt{15} \end{pmatrix},$$

$$M_3 = \frac{1}{4\sqrt{123}} \begin{pmatrix} 7\sqrt{5} & 12\sqrt{2} \\ -\sqrt{42} & 4\sqrt{105} \\ -41 & 0 \end{pmatrix}, \quad M_4 = \frac{1}{16\sqrt{3}} \begin{pmatrix} -7\sqrt{3} & -\sqrt{70} & 5\sqrt{15} \\ \sqrt{6} & -2\sqrt{35} & -3\sqrt{30} \\ -\sqrt{55} & -\sqrt{462} & -\sqrt{11} \end{pmatrix}. \quad (\text{A30})$$

e.  $\tilde{J} = 13/2$

$$\begin{aligned} & \left( \left| \Gamma_6, -\frac{1}{2} \right\rangle, \left| \Gamma_6, +\frac{1}{2} \right\rangle, \left| \Gamma_7^{(1)}, -\frac{1}{2} \right\rangle, \left| \Gamma_7^{(2)}, -\frac{1}{2} \right\rangle, \left| \Gamma_7^{(1)}, +\frac{1}{2} \right\rangle, \left| \Gamma_7^{(2)}, +\frac{1}{2} \right\rangle, \left| \Gamma_8^{(1)}, -\frac{1}{2} \right\rangle, \left| \Gamma_8^{(2)}, -\frac{1}{2} \right\rangle, \right. \\ & \quad \left. \left| \Gamma_8^{(1)}, +\frac{1}{2} \right\rangle, \left| \Gamma_8^{(2)}, +\frac{1}{2} \right\rangle, \left| \Gamma_8^{(1)}, -\frac{3}{2} \right\rangle, \left| \Gamma_8^{(2)}, -\frac{3}{2} \right\rangle, \left| \Gamma_8^{(1)}, +\frac{3}{2} \right\rangle, \left| \Gamma_8^{(2)}, +\frac{3}{2} \right\rangle \right) \\ & = \left( \left| +\frac{7}{2} \right\rangle, \left| -\frac{1}{2} \right\rangle, \left| -\frac{9}{2} \right\rangle, \left| -\frac{7}{2} \right\rangle, \left| +\frac{1}{2} \right\rangle, \left| +\frac{9}{2} \right\rangle, \left| -\frac{13}{2} \right\rangle, \left| -\frac{5}{2} \right\rangle, \left| +\frac{3}{2} \right\rangle, \left| +\frac{11}{2} \right\rangle, \right. \\ & \quad \left. \left| +\frac{13}{2} \right\rangle, \left| +\frac{5}{2} \right\rangle, \left| -\frac{3}{2} \right\rangle, \left| -\frac{11}{2} \right\rangle \right) \\ & \times \begin{pmatrix} M_1 & 0 & 0 & 0 & M_3 R^{(2)}(\beta) & 0 & 0 & 0 \\ 0 & M_1 & 0 & 0 & 0 & -M_3 R^{(2)}(\beta) & 0 & 0 \\ 0 & 0 & M_2 R^{(2)}(\alpha) & 0 & 0 & 0 & 0 & -M_4 M_3 R^{(2)}(\beta) \\ 0 & 0 & 0 & M_2 R^{(2)}(\alpha) & 0 & 0 & M_4 M_3 R^{(2)}(\beta) & 0 \end{pmatrix}, \quad (\text{A31}) \end{aligned}$$

where,

$$M_1 = \frac{1}{4} \begin{pmatrix} \sqrt{3} \\ -\sqrt{2} \\ \sqrt{11} \end{pmatrix}, \quad M_2 = \frac{1}{4\sqrt{114}} \begin{pmatrix} 4\sqrt{10} & -\sqrt{429} \\ -2\sqrt{286} & \sqrt{15} \\ 0 & 19\sqrt{3} \\ 2\sqrt{130} & 3\sqrt{33} \end{pmatrix},$$

$$M_3 = \frac{1}{4\sqrt{5}} \begin{pmatrix} \sqrt{33} & 4\sqrt{2} \\ -\sqrt{22} & 4\sqrt{3} \\ -5 & 0 \end{pmatrix}, \quad M_4 = \frac{1}{16\sqrt{6}} \begin{pmatrix} -\sqrt{143} & -\sqrt{858} & -\sqrt{39} \\ 5\sqrt{5} & -3\sqrt{30} & -\sqrt{165} \\ -21 & -5\sqrt{6} & \sqrt{33} \\ 7\sqrt{11} & -\sqrt{66} & -9\sqrt{3} \end{pmatrix}. \quad (\text{A32})$$

f.  $\tilde{J} = 15/2$

$$\begin{aligned} & \left( \left| \Gamma_6, -\frac{1}{2} \right\rangle, \left| \Gamma_6, +\frac{1}{2} \right\rangle, \left| \Gamma_7, -\frac{1}{2} \right\rangle, \left| \Gamma_7, +\frac{1}{2} \right\rangle, \left| \Gamma_8^{(1)}, -\frac{1}{2} \right\rangle, \left| \Gamma_8^{(2)}, -\frac{1}{2} \right\rangle, \left| \Gamma_8^{(3)}, -\frac{1}{2} \right\rangle, \left| \Gamma_8^{(1)}, +\frac{1}{2} \right\rangle, \right. \\ & \quad \left. \left| \Gamma_8^{(2)}, +\frac{1}{2} \right\rangle, \left| \Gamma_8^{(3)}, +\frac{1}{2} \right\rangle, \left| \Gamma_8^{(1)}, -\frac{3}{2} \right\rangle, \left| \Gamma_8^{(2)}, -\frac{3}{2} \right\rangle, \left| \Gamma_8^{(3)}, -\frac{3}{2} \right\rangle, \left| \Gamma_8^{(1)}, +\frac{3}{2} \right\rangle, \left| \Gamma_8^{(2)}, +\frac{3}{2} \right\rangle, \left| \Gamma_8^{(3)}, +\frac{3}{2} \right\rangle \right) \\ & = \left( \left| +\frac{15}{2} \right\rangle, \left| +\frac{7}{2} \right\rangle, \left| -\frac{1}{2} \right\rangle, \left| -\frac{9}{2} \right\rangle, \left| -\frac{15}{2} \right\rangle, \left| -\frac{7}{2} \right\rangle, \left| +\frac{1}{2} \right\rangle, \left| +\frac{9}{2} \right\rangle, \right. \\ & \quad \left. \left| -\frac{13}{2} \right\rangle, \left| -\frac{5}{2} \right\rangle, \left| +\frac{3}{2} \right\rangle, \left| +\frac{11}{2} \right\rangle, \left| +\frac{13}{2} \right\rangle, \left| +\frac{5}{2} \right\rangle, \left| -\frac{3}{2} \right\rangle, \left| -\frac{11}{2} \right\rangle \right) \\ & \times \begin{pmatrix} M_1 & 0 & 0 & 0 & M_3 R^{(3)}(\Omega) & 0 & 0 & 0 \\ 0 & -M_1 & 0 & 0 & 0 & M_3 R^{(3)}(\Omega) & 0 & 0 \\ 0 & 0 & M_2 & 0 & 0 & 0 & 0 & M_4 M_3 R^{(3)}(\Omega) \\ 0 & 0 & 0 & -M_2 & 0 & 0 & M_4 M_3 R^{(3)}(\Omega) & 0 \end{pmatrix}, \quad (\text{A33}) \end{aligned}$$

where,

$$\begin{aligned}
 M_1 &= -\frac{1}{8\sqrt{3}} \begin{pmatrix} \sqrt{65} \\ \sqrt{21} \\ \sqrt{99} \\ \sqrt{7} \end{pmatrix}, \quad M_2 = \frac{1}{8\sqrt{3}} \begin{pmatrix} \sqrt{77} \\ \sqrt{65} \\ -\sqrt{39} \\ -\sqrt{11} \end{pmatrix}, \quad M_3 = \frac{1}{24\sqrt{19}} \begin{pmatrix} -2\sqrt{266} & -2\sqrt{1430} & -\sqrt{455} \\ 0 & 0 & 57\sqrt{3} \\ 0 & 48\sqrt{2} & -3\sqrt{77} \\ 2\sqrt{2470} & -2\sqrt{154} & -7 \end{pmatrix}, \\
 M_4 &= \frac{1}{64\sqrt{3}} \begin{pmatrix} \sqrt{15} & 7\sqrt{91} & -\sqrt{429} & -3\sqrt{273} \\ \sqrt{3003} & -7\sqrt{55} & -3\sqrt{105} & 3\sqrt{165} \\ \sqrt{5005} & -\sqrt{33} & -15\sqrt{7} & -17\sqrt{11} \\ \sqrt{105} & 17\sqrt{13} & -\sqrt{3003} & 11\sqrt{39} \end{pmatrix}.
 \end{aligned} \tag{A34}$$

TABLE IV. Coefficients  $v_{k,|q|}$  in Eq. (C1).

$k$	$v_{k,0}$	$v_{k,4}$	$v_{k,8}$	$v_{k,12}$	$v_{k,16}$
4	1	$\sqrt{\frac{5}{14}}$			
6	1	$-\sqrt{\frac{7}{2}}$			
8	1	$\frac{1}{3}\sqrt{\frac{14}{11}}$	$\frac{1}{3}\sqrt{\frac{65}{22}}$		
10	1	$-\sqrt{\frac{66}{65}}$	$-\sqrt{\frac{187}{130}}$		
12	1	0	$\sqrt{\frac{429}{646}}$	$4\sqrt{\frac{91}{7429}}$	
	0	1	$-4\sqrt{\frac{42}{323}}$	$9\sqrt{\frac{11}{7429}}$	
14	1	$-\frac{3}{2}\sqrt{\frac{143}{595}}$	$-\sqrt{\frac{741}{1190}}$	$-\frac{1}{2}\sqrt{\frac{437}{119}}$	
16	1	0	$\sqrt{\frac{442}{2185}}$	$\frac{16}{5}\sqrt{\frac{17}{437}}$	$7\sqrt{\frac{493}{135470}}$
	0	1	$-6\sqrt{\frac{6}{805}}$	$-\frac{31}{5}\sqrt{\frac{13}{483}}$	$4\sqrt{\frac{754}{74865}}$

### Appendix B: Decomposition of operator

An operator  $\hat{A}$  acting on the electronic states from  $\mathcal{H}$  (1) is decomposed into the irreducible tensor operators (8):

$$\hat{A} = \sum_{kq} a_{kq} \mathcal{Y}_{kq}. \tag{B1}$$

Here,  $\tilde{\mathcal{J}}$  is omitted for simplicity from the argument of  $\mathcal{Y}_{kq}$ , and the coefficients  $a_{kq}$  are calculated as

$$a_{kq} = (-1)^q \frac{[k]}{[\tilde{\mathcal{J}}]} \left[ \langle (\tilde{\mathcal{J}}k) \tilde{\mathcal{J}} \tilde{\mathcal{J}} | \tilde{\mathcal{J}} \tilde{\mathcal{J}} k 0 \rangle \right]^2 \text{Tr} \left[ \mathcal{Y}_{k,-q} \hat{A} \right], \tag{B2}$$

$[x] = 2x + 1$ , and Tr is the trace over  $\mathcal{H}$ . The irreducible tensor operators  $\mathcal{Y}_{kq}$  are written in slightly different form

compared to conventional Stevens operators [37]. The advantages of the current form are that (a) explicit form of the Stevens operators is not necessary (only easily obtainable Clebsch-Gordan coefficients are necessary), (b) it is suitable form for the use of group theoretical techniques, and (c) the coefficients  $a_{kq}$  directly indicate the strength of the contribution because the magnitude of  $\mathcal{Y}_{kq}$  is expected to be of the order of unity.

### Appendix C: The form of the crystal field

The totally symmetric  $k$ -th rank tensor of cubic group is expressed as

$$\begin{aligned}
 \hat{V}_k &= v_{k,0} \mathcal{Y}_{k0} + \sum_{q=\pm 4} v_{k,4} \mathcal{Y}_{kq} + \sum_{q=\pm 8} v_{k,8} \mathcal{Y}_{kq} \\
 &+ \sum_{q=\pm 12} v_{k,12} \mathcal{Y}_{kq} + \sum_{q=\pm 16} v_{k,16} \mathcal{Y}_{kq}.
 \end{aligned} \tag{C1}$$

The coefficients  $v_{k,|q|}$  listed in Table IV are determined by making use of the fact that Eq. (C1) is invariant under  $C_4^y$  and  $C_4^z$  rotations. The 12th and 16th order operators contain two independent sets of coefficients which are shown in different lines in Table IV. The crystal field Hamiltonian is a linear combination of Eq. (C1):

$$\hat{H}_{\text{cf}} = \sum_k B_k \hat{V}_k. \tag{C2}$$

$B_0$  is the average of the crystal-field energies. There is one  $B_k$  for each rank  $k = 4, 6, 8, 10, 14$  and there are two  $B_k$  for each  $k = 12, 16$ .

- [1] H. A. Bethe, "Splitting of Terms in Crystals," Ann. Physik **3**, 133 (1929).  
 [2] A. Abragam and B. Bleaney, *Electron Paramagnetic Resonance of Transition Ions* (Clarendon Press, Oxford, 1970).

- [3] G. H. Dieke, *Spectra and Energy Levels of Rare-Earth Ions in Crystals* (Academic Press Inc., New York, 1967).  
 [4] N. Ishikawa, M. Sugita, T. Ishikawa, S. Koshihara, and Y. Kaizu, "Lanthanide Double-Decker Complexes Functioning as Magnets at the Single-Molecular Level," J.

- Am. Chem. Soc. **125**, 8694 (2003).
- [5] N. Magnani, P. Santini, G. Amoretti, and R. Caciuffo, "Perturbative approach to  $J$  mixing in  $f$ -electron systems: Application to actinide dioxides," *Phys. Rev. B* **71**, 054405 (2005).
- [6] J. F. McNulty, B. J. Ruck, and H. J. Trodahl, "On the ferromagnetic ground state of SmN," *Phys. Rev. B* **93**, 054413 (2016).
- [7] M. Ruminy, E. Pomjakushina, K. Iida, K. Kamazawa, D. T. Adroja, U. Stuhr, and T. Fennell, "Crystal-field parameters of the rare-earth pyrochlores  $R_2\text{Ti}_2\text{O}_7$  ( $R = \text{Tb}, \text{Dy}, \text{and Ho}$ )," *Phys. Rev. B* **94**, 024430 (2016).
- [8] J. H. Van Vleck, "Valence strength and the magnetism of complex salts," *J. Chem. Phys.* **3**, 807 (1935).
- [9] C. K. Jørgensen, R. Pappalardo, and H.-H. Schmidtke, "Do the "ligand field" parameters in lanthanides represent weak covalent bonding?" *J. Chem. Phys.* **39**, 1422 (1963).
- [10] R. E. Watson and A. J. Freeman, "Covalent Effects in Rare-Earth Crystal-Field Splittings," *Phys. Rev.* **156**, 251 (1967).
- [11] N. A. Bogdanov, V. M. Katukuri, J. Romhányi, V. Yushankhai, V. Kataev, B. Büchner, J. van den Brink, and L. Hozoi, "Orbital reconstruction in nonpolar tetravalent transition-metal oxide layers," *Nat. Commun.* **6**, 7306 (2015).
- [12] E. Lefrançois, A.-M. Pradipto, M. Moretti Sala, L. C. Chapon, V. Simonet, S. Picozzi, P. Lejay, S. Petit, and R. Ballou, "Anisotropic interactions opposing magnetocrystalline anisotropy in  $\text{Sr}_3\text{NiIrO}_6$ ," *Phys. Rev. B* **93**, 224401 (2016).
- [13] L. F. Chibotaru, A. Ceulemans, and H. Bolvin, "Unique Definition of the Zeeman-Splitting  $g$  Tensor of a Kramers Doublet," *Phys. Rev. Lett.* **101**, 033003 (2008).
- [14] L. F. Chibotaru and L. Ungur, "*Ab initio* calculation of anisotropic magnetic properties of complexes. I. Unique definition of pseudospin Hamiltonians and their derivation," *J. Chem. Phys.* **137**, 064112 (2012).
- [15] L. F. Chibotaru, "*Ab Initio* Methodology for Pseudospin Hamiltonians of Anisotropic Magnetic Complexes," in *Adv. Chem. Phys.*, Vol. 153, edited by S. A. Rice and A. R. Dinner (John Wiley & Sons, New Jersey, 2013) pp. 397–519.
- [16] L. F. Chibotaru, L. Ungur, and A. Soncini, "The Origin of Nonmagnetic Kramers Doublets in the Ground State of Dysprosium Triangles: Evidence for a Toroidal Magnetic Moment," *Angew. Chem. Int. Ed.* **120**, 4194 (2008).
- [17] L. F. Chibotaru, "Theoretical Understanding of Anisotropy in Molecular Nanomagnets," in *Molecular Nanomagnets and Related Phenomena*, Struct. Bond., Vol. 164, edited by S. Gao (Springer Berlin Heidelberg, 2015) pp. 185–229.
- [18] L. Ungur, J. J. LeRoy, I. Korobkov, M. Murugesu, and L. F. Chibotaru, "Fine-tuning the Local Symmetry to Attain Record Blocking Temperature and Magnetic Remanence in a Single-Ion Magnet," *Angew. Chem. Int. Ed.* **53**, 4413 (2014).
- [19] L. Ungur and L. F. Chibotaru, "Strategies toward High-Temperature Lanthanide-Based Single-Molecule Magnets," *Inorg. Chem.* **55**, 10043 (2016).
- [20] L. Ungur and L. F. Chibotaru, "*Ab Initio* Crystal Field for Lanthanides," *Chem. Eur. J.* **23**, 3708 (2017).
- [21] N. Iwahara, V. Vieru, L. Ungur, and L. F. Chibotaru, "Zeeman interaction and Jahn-Teller effect in the  $\Gamma_8$  multiplet," *Phys. Rev. B* **96**, 064416 (2017).
- [22] Since pure spin/orbital/total angular momentum operators do not commute with the Hamiltonian of materials due to the coexistence of crystal-field and spin-orbit coupling, the "spin" operators in phenomenological model are not pure ones but correspond to pseudo (effective, fictitious) spin (see Sec. 1.4 and 3.1 in Ref. [2]).
- [23] In order to fulfill time-reversal symmetry, it is necessary to generate integer and half-integer pseudospin states for non-Kramers and Kramers systems, respectively. However, sometimes half-integer pseudospin is used to describe (quasi) degenerate state of non-Kramers system for simple description of the Hamiltonian. Care is needed in this case because not all symmetry properties are fulfilled, therefore, its unusual behaviour might be expected. For example, double degenerate  $\Gamma_3$  states never transform as  $\Gamma_6$  ( $S = 1/2$  spin) states in cubic group. Even if the pseudospin states are enforced to fulfill the time-reversal symmetry, the crystal-field Hamiltonian contains odd order terms of pseudospin operator [38].
- [24] P. W. Anderson, *Basic Notions of Condensed Matter Physics* (Benjamin-Cummings, Menlo Park, 1984).
- [25] R. B. Laughlin, "Nobel Lecture: Fractional quantization," *Rev. Mod. Phys.* **71**, 863 (1999).
- [26] N. M. Edelstein and G. H. Lander, "Magnetic properties," in *The Chemistry of the Actinide and Transactinide Elements, 3rd ed.*, edited by L. R. Morss, N. M. Edelstein, and J. Fuger (Springer, Dordrecht, 2006) pp. 2225–2306.
- [27] G. F. Koster, J. O. Dimmock, R. G. Wheeler, and H. Statz, *Properties of the thirty-two point groups* (MIT press, Massachusetts, 1963).
- [28] D. A. Varshalovich, A. N. Moskalev, and V. K. Khersonskii, *Quantum Theory of Angular Momentum* (World Scientific, Singapore, 1988).
- [29] R. Huby, "Phase of Matrix Elements in Nuclear Reactions and Radioactive Decay," *Proc. Phys. Soc. A* **67**, 1103 (1954).
- [30] K. R. Lea, M. J. M. Leask, and W. P. Wolf, "The raising of angular momentum degeneracy of  $f$ -Electron terms by cubic crystal fields," *J. Phys. Chem. Solids* **23**, 1381 (1962).
- [31] X. Zhou, C. S. K. Mak, P. A. Tanner, and M. D. Faucher, "Spectroscopic properties and configuration interaction assisted crystal field analysis of  $\text{Nd}^{3+}$  in neat  $\text{Cs}_2\text{NaNdCl}_6$ ," *Phys. Rev. B* **73**, 075113 (2006).
- [32] E. R. Bernstein and L. W. Dennis, "Electron-paramagnetic-resonance data interpretation for a  $\Gamma_8(O_h)$  state in a cubic crystal field," *Phys. Rev. B* **20**, 870 (1979).
- [33] N. Edelstein, W. Kolbe, and J. E. Bray, "Electron paramagnetic resonance spectrum of the  $\Gamma_8$  ground state of  $\text{Np}^{4+}$  diluted in  $\text{Cs}_2\text{ZrCl}_6$ ," *Phys. Rev. B* **21**, 338 (1980).
- [34] A. A. Granovsky, "Extended multi-configuration quasi-degenerate perturbation theory: The new approach to multi-state multi-reference perturbation theory," *J. Chem. Phys.* **134** (2011).
- [35] T. Shiozaki, W. Györfly, P. Celani, and H.-J. Werner, "Communication: Extended multi-state complete active space second-order perturbation theory: Energy and nuclear gradients," *J. Chem. Phys.* **135** (2011).
- [36] F. Aquilante, J. Autschbach, R. K. Carlson, L. F. Chibotaru, M. G. Delcey, L. De Vico, I. Fdez. Galván, N. Ferré, L. M. Frutos, L. Gagliardi, M. Garavelli, A. Giussani, C. E. Hoyer, G. Li Manni, H. Lischka, D. Ma, P.-Å.

Malmqvist, T. Müller, A. Nenov, M. Olivucci, T. B. Pedersen, D. Peng, F. Plasser, B. Pritchard, M. Reiher, I. Rivalta, I. Schapiro, J. Segarra-Martí, M. Stenrup, D. G. Truhlar, L. Ungur, A. Valentini, S. Vancoillie, V. Veryazov, V. P. Vysotskiy, O. Weingart, F. Zapata, and R. Lindh, “Molcas 8: New capabilities for multi-configurational quantum chemical calculations across the

- periodic table,” *J. Comput. Chem.* **37**, 506 (2016).
- [37] K. W. H. Stevens, “Matrix Elements and Operator Equivalents Connected with the Magnetic Properties of Rare Earth Ions,” *Proc. Phys. Soc. London, Sec. A* **65**, 209 (1952).
- [38] K. A. Mueller, “Effective-Spin Hamiltonian for “Non-Kramers” Doublets,” *Phys. Rev.* **171**, 350 (1968).